Isospin dependent thermodynamics of fragmentation

Ad. R. Raduta
NIPNE, Bucharest-Magurele, POB-MG 6, Romania and
Institut de Physique Nucleaire, IN2P3-CNRS, F-91406 Orsay Cedex, France

F. Gulminelli*
LPC (IN2P3-CNRS/Ensicaen et Université), F-14050 Caen Cedex, France
(Received 15 November 2006; revised manuscript received 14 February 2007; published 18 April 2007)

The thermal and phase properties of a multifragmentation model that uses clusters as degrees of freedom are explored as a function of isospin. Good qualitative agreement is found with the phase diagram of asymmetric nuclear matter as established by different mean-field models. In particular, from the convexity properties of the nuclear entropy, we show that uncharged finite nuclei display first- and second-order liquid-gas-like phase transitions. Different quantities are examined to connect the thermal properties of the system to cluster observables. In particular, we show that fractionation is only a loose indication of phase coexistence. A simple analytical formula is proposed and tested to evaluate the symmetry (free) energy from the widths of isotopic distributions. Assuming that one may restore the isotopic composition of breakup fragments, it is found that some selected isotopic observables can allow one to quantitatively access the freeze-out symmetry energy in multifragmentation experiments.

DOI: 10.1103/PhysRevC.75.044605 PACS number(s): 25.70.Pq, 24.10.Pa

I. INTRODUCTION

Due to the short-range repulsive and finite-range attractive character of the nucleon-nucleon interaction, nuclear matter is known to exhibit a phase transition similar to the liquid-gas transition taking place in real fluids [1,2].

Many experimental and theoretical efforts have been devoted to this subject [3]; in particular, most recent works focus on asymmetric matter and the effect of isospin as an additional degree of freedom [4–7]. Mean-field-based models have demonstrated the presence of a first-order phase transition in both isospin symmetric and asymmetric nuclear matter [8], the decrease of the critical temperature with increasing isospin asymmetry, and, in the case of asymmetric matter, different neutron-proton compositions of the liquid and gas phases [4,6–8].

In astrophysics, both neutron-star structure and supernova dynamics are influenced by thermal properties of neutron-rich nuclear matter in a large interval of temperatures and densities [9,10]. All these different phenomena involve excited matter at baryon densities lower than normal nuclear matter density; this corresponds in the phase diagram to a region of instability with respect to phase separation. Information on the phase structure and properties of hot and diluted nuclear matter is thus clearly of astrophysical relevance.

From an experimental point of view, the only terrestrial phenomenon that may allow one to access finite-temperature low-density properties of neutron-rich matter and, in particular, to pin down the density and temperature dependence of the symmetry energy is given by nuclear multifragmentation [3]. Indeed, this specific decay channel of nuclei, whose excitation energy is of the order of a few MeV/nucleon, has for a long time been tentatively associated with the coexistence zone of the nuclear matter phase diagram [11].

However, the connection between multifragmentation observables and the nuclear matter energy-density functional and phase structure is far from being trivial. First, finite nuclei are charged, whereas nuclear matter is by definition neutral. Therefore, the presence of this nonsaturating long-range force makes it difficult to relate the multifragmentation phenomenology to the theoretical studies of nuclear matter [1]. Second, and even more important, atomic nuclei are composed of a very small number of constituents, and their phase properties are not trivially linked to the phase structure of nuclear matter. At the thermodynamic limit, the coexistence zone is a simple linear superposition of pure liquid and gas phases, and it can be deduced from a mean-field approach through a Gibbs construction. The situation is completely different in finite nuclei, where phase coexistence is revealed by convexity anomalies of the entropy surface [13,14]. The properties of coexistence cannot be deduced from the properties of the pure phases (nuclei and nucleons, respectively), mean-field based approaches badly fail, and a description explicitly accounting for complex clusterization is mandatory [13].

A typical example of this ambiguity is given by the fractionation phenomenon, originally expounded as a consequence of Gibbs phase equilibrium, later recognized as a generic feature of cluster formation [15–17], and systematically observed

*Member of the Institut Universitaire de France.

[1]It is interesting to note that, on the other hand, the presence of the Coulomb interaction may make finite nuclei a good laboratory in which to address the properties of compact stellar objects. Indeed, neutrality is verified only on a macroscopic scale in neutron star crust matter, and charge fluctuations are recognized to be at the origin of the crust phase structure [12].

in experimental analyses [18–22]: a clear thermodynamic interpretation of fractionation is not trivial in a finite system, because we cannot unambiguously associate a given fragment size to the "liquid" or "gas" phase.

To contribute to closing the gap between nuclear matter thermodynamic studies and nuclear multifragmentation, we investigate in this paper the isospin dependent phase diagram of finite excited nuclei. The study is done in the framework of the microcanonical multifragmentation model (MMM) [23], which explicitly considers clusters as degrees of freedom. A similar analysis was already presented in Ref. [24], where Coulomb effects on the phase diagram were especially addressed. Here, in order to concentrate on isospin effects, we first consider that the Coulomb interaction is switched off. The use of such an idealized neutral system will additionally allow us to make connections with the expected behavior at the thermodynamic limit and to explore the link between isospin observables (isoscaling [16,22,25–29], isospin fluctuations [18,22,30–32]) and the low-density finite-temperature symmetry (free) energy of the equation of state. The robustness of measurements of the symmetry energy in both finite neutral systems and real nuclei under the effect of mass and charge conservation and Coulomb is finally addressed.

II. THEORETICAL FRAMEWORK

To provide a realistic description of multifragment production, a theory dealing with complex correlations well beyond the mean field is needed. An exact solution of this problem at the microscopic level is provided by classical models (molecular dynamics, lattice gas) [11], which, however, completely miss all the specific quantal features of the process. Moreover, no connection is possible within these models between fragment observables and the different ingredients of the nuclear energy-density functional, which are explored through multifragmentation reactions. On the other hand, semiclassical or quantum molecular models (such as QMD [33], AMD [34]) which reproduce the most important macroscopic nuclear properties as density distributions and binding energies, and account for nucleon-nucleon interaction and Pauli blocking, still do not offer a definite description of multifragmentation and access to the equation of state of excited matter because of the ambiguity of the fragments and breakup definition.

An interesting alternative is given by statistical models which use clusters as degrees of freedom [35]. Such models offer the remarkable advantage that all nuclear bound as well as continuum states are naturally accounted for via empirical parametrizations of the cluster energies and level densities, allowing a direct comparison with experimental data.

The price to pay for such a realistic inclusion of nuclear effects is the underlying hypothesis that nuclear correlations are entirely exhausted by clusterization, which amounts to the implementation of the properties of isolated low excited nuclei for the description of breakup fragments. This limitation can in principle be avoided by including effective in-medium corrections in the fragment energy functional [36]. In this case, however, the fragment energy becomes a free parameter of the theory.

The distinctive feature of the fragmentation process, namely, the explosion of an isolated nucleus into a vacuum, recommends the microcanonical framework [37–39] as the most natural choice. The nonphysical hypothesis of a sharp fixed freeze-out volume constraint may be easily overcome by considering a total spatial extension for the fragmenting system fluctuating event by event [40]. Technically, this is realized by introducing a λ Lagrange parameter conjugate of the volume V which alters the statistical weight of a configuration W_C by an extra factor, $\exp(-\lambda V)$ [41]. The thermodynamical potential associated with this ensemble is $\bar{S}_E[\lambda] = S - \lambda V = \ln \mathcal{W}(E, \lambda)$, where $\mathcal{W}(E, \lambda) = \int W(E, V) \exp(-\lambda V)\, \mathrm{dV}$. In addition, for a system belonging to the liquid-gas universality class, the exploration of the configuration space along constant λ paths provides a straightforward method to reveal phase coexistence by the back bending of the corresponding caloric curves and to finally construct the phase diagram [14].

The MMM version [23] of the microcanonical multifragmentation models [37–39] has been used so far to investigate the thermodynamic properties of charged nuclei with excitation energies between 1 and 15 MeV/nucleon [24] and will be presently employed for the study of isospin effects. MMM provides a Monte Carlo calculation of the global density of states $W(A, Z, E, \boldsymbol{P}, \boldsymbol{L}, V)$ of a nuclear system modeled as a noninteracting collection of nuclear clusters. The space of observables is given by the baryonic number A, proton number Z, total energy E, total momentum $\boldsymbol{P}$, total angular momentum $\boldsymbol{L}$, and freeze-out volume V. The investigation of all cluster states compatible with conservation laws and geometrical restrictions is performed using a Metropolis trajectory in configuration space.

Breakup fragments are considered as having normal nuclear density ρ_0 and described by a ground-state liquid-drop binding energy including surface and symmetry terms. This description is consistent with a semiclassical Thomas-Fermi approximation [42] or hot Hartree-Fock [43], where the effect of temperature is a modified occupation of the single-particle eigenstates of the mean-field Hamiltonian. The finite-temperature fragment energy functional in this approach is thus modified with respect to the ground state only for the internal excitation energy (ϵ) coming from the occupation of continuum states, which are treated with a Fermi gas level density parametrization. To avoid double counting of the free particle states [44], a high energy cutoff ($\tau = 9$ MeV) is applied to the level density.

To allow comparison with the well-known nuclear matter thermodynamics [4,6,8] and to best isolate isospin effects on the fragmentation process, we ignore the long-range Coulomb interaction, and to avoid interference with finite size effects, we consider equal size systems which differ by the neutron-proton ratio.

III. PHASE DIAGRAM

The isospin dependence of the phase diagram for the MMM model is easily spotted in the microcanonical "isobar" ensemble, where energy is fixed and volume fluctuations

are allowed and controlled through a conjugated Legendre intensive.

Indeed, contrary to ordinary (macroscopic) thermodynamics, the thermal and phase characteristics of a finite system depend on the statistical ensemble considered. The liquid-gas phase transition has a nonzero latent heat and has density as an order parameter, meaning that the two associated phases can be distinguished by their different particle and energy densities. If a finite system (with a given fixed particle number) exhibits this transition, its event distribution at the transition point will show the two peaks corresponding to the two phases if and only if both energy and volume are free to fluctuate, i.e., in the canonical isobar ensemble [14].

The general relationship between a distribution in the ensemble characterized by an intensive variable γ associated with the conjugated extensive variable m, and the Boltzmann entropy $W(m) = \exp S(m)$,

$$P_\gamma(m) = Z_\gamma^{-1} \exp\,(S(m) - \gamma m), \tag{1}$$

ensures then that at the liquid-gas transition point, the compressibility is negative in the canonical isochore (β, V) ensemble, and the heat capacity is negative in the microcanonical isobar (E, P) ensemble.

In the multifragmentation transition described by MMM, the low multiplicity ordered phase (compound nucleus) and high multiplicity disordered phase (multifragmentation) can be distinguished by their energy and volume, just like in regular liquid-gas systems, and all the above considerations apply [24].

Figure 1 shows some constant λ microcanonical caloric curves of 200-nucleon systems with different neutron-proton ratios. The Lagrange parameter λ can be associated with a pressure through $P = \lambda T$, where $T = (\partial \bar{S}_E[\lambda]/\partial E)^{-1}$ is the constant λ microcanonical temperature. The expected isospin invariance in the absence of the Coulomb interaction is confirmed by the fact that mirror nuclei [(200,70) vs (200,130), and (200,50) vs (200,150)] show an identical thermodynamical behavior, translated into fully superimposable caloric curves.

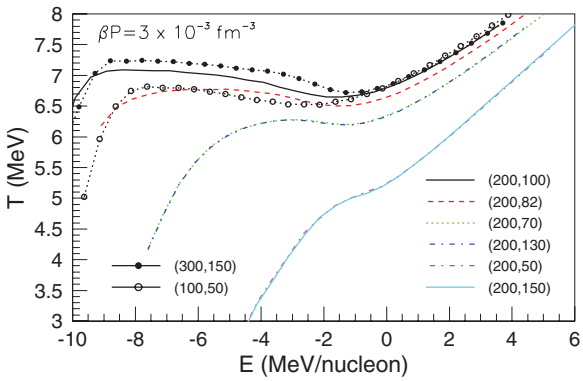

FIG. 1. (Color online) Microcanonical caloric curves at constant $\lambda = (\beta P) = 3 \times 10^{-3}$ fm^{-3} for 200-nucleon systems and various neutron-proton ratios as indicated in the legend. E is the total energy of the system. The magnitude of finite size effects with respect to isospin ones may be estimated considering the caloric curves with the same value of λ corresponding to the symmetric nuclei (100,50) and (300,150).

The symmetric system shows a broad back bending, signaling a liquid-gas-like phase transition. Increasing the isospin asymmetry, the temperature shows a monotonic decrease, and the back-bending width shrinks. The λ value, $\lambda = 3 \times 10^{-3}$ fm^{-3}, which still corresponds to the coexistence region for the $Z/A = 0.35$ system, appears clearly supercritical for $Z/A = 0.25$.

The presence of Coulomb effects in physical nuclear systems breaks the n-p invariance and can considerably mask the isospin effects shown by Fig. 1 [24]. To disentangle these effects, most of the experimental analyses concentrate on different isotopes of the same element (e.g., ^{112}Sn+^{112}Sn and ^{124}Sn+^{124}Sn collisions). In this case, however, the sources have different total sizes, and a naturally rising question is to what extent finite size effects interfering with asymmetry effects may blur the signals of the last ones. A quantitative answer is offered by Fig. 1, where caloric curves corresponding to symmetric systems 50% larger and 50% smaller than the previously discussed ones are considered. The relative displacement of the curves suggests that for most of the presently analyzed multifragmentation reactions, finite size effects are small enough to be safely negligible.

The monotonic decrease of the critical temperature and pressure with the isospin asymmetry, together with the reduction of the coexistence region, are illustrated in Fig. 2, where the phase diagrams of 200-nucleon systems with different asymmetries are projected in the temperature–total-energy, pressure-temperature, and pressure–total-energy planes. The solid lines correspond to the borders of the coexistence region, obtained from a Maxwell construction on the constant λ microcanonical caloric curves. The dashed lines indicate the borders of the spinodal zone, defined by the back-bending extension for each λ value. The thick solid line connects the critical points in any representation. By extrapolating this line, we can see that pure neutron and proton systems may exist only in the supercritical phase, as expected from their inability to form clusters at any temperature. It is interesting to note that this intuitive result is obtained only as a limiting situation, while a phase transition survives with a sizable critical temperature for systems as asymmetric as $Z/A = 0.25$.

These results are in qualitative agreement with nuclear matter calculations [4,6,8], showing that the thermodynamics of fragmentation of a finite nuclear system can be associated with the phenomenology of the nuclear matter liquid-gas phase transition. This intuitive connection is systematically pushed forward in experimental studies; however, from a theoretical point of view, this is not a trivial issue. Caloric curves and heat capacities in the statistical multifragmentation model (SMM) have been available for more than two decades, and most calculations with finite systems [38] have been performed at constant volume and not constant pressure, thus leading to signals that cannot univocally be interpreted as a first-order phase transition. A detailed exploration of the fragmentation phase diagram was presented in Refs. [3,45]. The results show a continuous transition from a high-temperature single phase to a mixed phase, this latter extending over the whole density domain of validity of the model [45]. This is reminiscent of

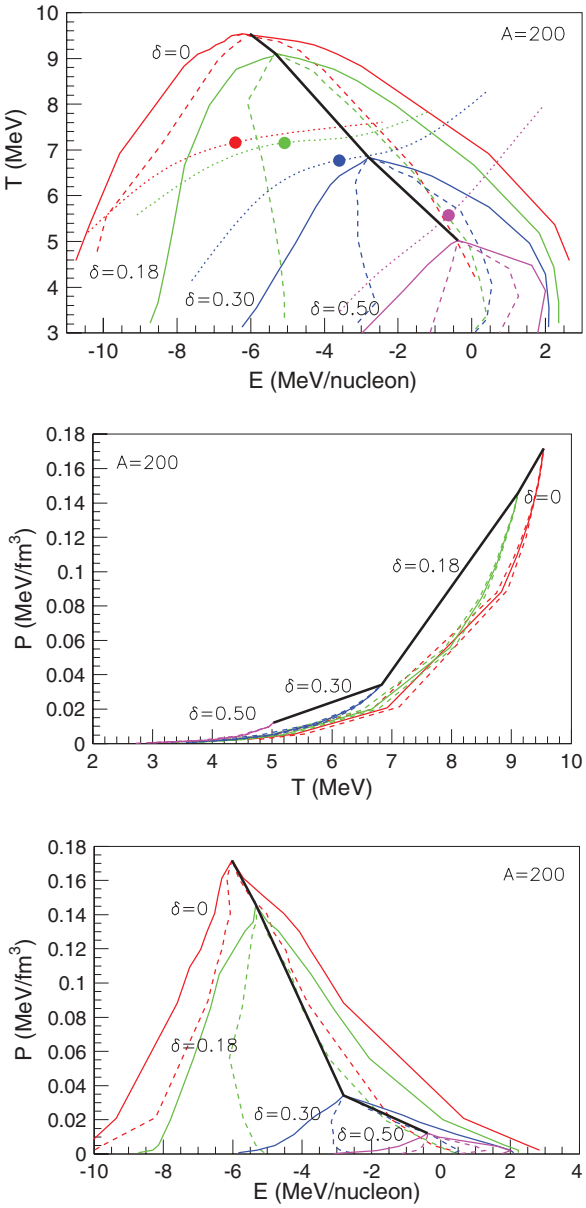

FIG. 2. (Color online) Projections in the temperature–total-energy, pressure-temperature, and pressure–total-energy planes of the phase diagrams of 200-nucleon systems with various isospin asymmetries ($\delta = (N\text{-}Z)/A = 0$, 0.18, 0.30 and 0.50). Solid lines mark the borders of the coexistence region, dashed lines indicate the borders of the spinodal zone. Dotted lines in the upper panel show the paths followed through the phase diagram by the considered systems when the average freeze-out volume is fixed to $6V_0$ and the excitation energy ranges from 2 to 10 MeV/nucleon. Solid symbols point the location of multifragmentation events with $E_{ex} =$ 6 MeV/nucleon.

liquid-gas phenomenology, but the transition from the liquid side, which is the only one accessible experimentally, cannot be studied within this analytical model and is presented here for the first time. The isospin dependence of the fragmentation phase diagram also has never been studied before to our knowledge.

IV. ISOTOPIC DISTRIBUTIONS AND FRACTIONATION

In this section, we turn to the connection between the system phase diagram and cluster observables.

The generic feature of a first-order fluid phase transition with two conserved particle numbers is the fractionation phenomenon: if the coupling between like particles is less attractive than the coupling between unlike ones, the ordered phase is systematically more symmetric than the disordered one. In the previous section, we showed that the fragmentation transition is qualitatively similar to such a fluid transition; we can therefore expect to find traces of fractionation in the fragment and particle chemical compositions.

Looking at the isotopic composition of fragments of different size emitted by neutron-rich nuclei, it has been observed that the isospin ratio A/Z is a monotonically decreasing function of the fragment size, as one would intuitively expect if fractionation takes place and thermodynamic discontinuities are rounded by finite size effects. This "fractionation" phenomenon has been observed not only in experimental analyses [18–22], but also in different dynamical models [15–17], where it does not always seem connected to the phase coexistence phenomenology.

As we stressed in Sec. I, when dealing with finite systems, the properties of coexisting phases cannot be deduced from the properties of pure phases by a simple linear combination. It is therefore not clear whether the neutron (proton) enrichment of the nuclear gas (liquid) characteristic of phase coexistence in neutron-rich nuclear matter [4,6,8] will be apparent in the partitions of the finite system inside the coexistence region.

Figure 3 presents isotopic yield distributions of isobars with $A = 6$, 15, 20, and 30 obtained in the multifragmentation of nuclear systems (200,100) [$\delta = (N - Z)/A = 0$], (200,82) ($\delta = 0.18$), (200,70) ($\delta = 0.30$), (200,50) ($\delta = 0.50$), (200,130) ($\delta = 0.30$), and (200,150) ($\delta = 0.50$) in a state representative of most multifragmentation reactions, $E_{ex} =$ 6 MeV/nucleon and $\langle V \rangle = 6V_0$, where V_0 is the volume corresponding to normal nuclear density; the free neutron and proton multiplicities are listed in Table I. These states are located in very different regions of the phase diagram. This is shown in the upper panel of Fig. 2, where the dotted lines mark the paths followed by the considered systems when the average volume is fixed to $\langle V \rangle = 6V_0$ and the excitation energy increases from 2 to 10 MeV/nucleon. We can see that the $\langle V \rangle = 6V_0$ and $E_{ex} = 6$ MeV/nucleon state (reported by solid circles) is situated well inside the spinodal zone for $\delta = 0$ and $\delta = 0.18$, while it is close to the critical point for $\delta = 0.30$ and belongs to the supercritical region for $\delta = 0.50$.

The distributions of Fig. 3 exhibit some trivial characteristic features: the isospin symmetric source produces preferentially isospin symmetric breakup fragments (the isotopic yield distributions have a maximum at $Z = A/2$), and breakup fragment formation is invariant to n-p inversion (neutron and proton yields are equal, and isotopic yield distributions are symmetric with respect to $A/2$). Concerning the isospin asymmetric systems, one can see that the more neutron (proton) rich is the source, the more free neutrons (protons) are emitted, and the more neutron (proton) rich are the breakup fragments. The isospin invariance in the absence of the Coulomb interaction is

TABLE I. Neutron and proton breakup multiplicity for different 200-nucleon systems with an excitation energy of 6 MeV/nucleon and average freeze-out volume $\langle V \rangle = 6V_0$.

Multiplicity/Source	(200,100)	(200,82)	(200,70)	(200,50)	(200,130)	(200,150)
Neutron	6.71	1.31×10^1	2.09×10^1	3.27×10^1	1.28	1.80×10^{-1}
Proton	6.71	3.10	1.27	1.80×10^{-1}	2.07×10^1	3.24×10^1

confirmed by the isotopic yield distribution of the mirror nuclei (200,70) vs (200,130) and (200,50) vs (200,150), which have reflection symmetry with respect to the $Z = A/2$ axis.

One can also notice that the distributions are cut, both on the proton-rich and on the neutron-rich side. This is due to the dramatic decrease of the binding energy with isospin asymmetry approaching the drip lines. As a consequence, for asymmetric sources, primary fragments tend to be more symmetric than the initial source, the total asymmetry of the system being preserved by a correspondingly increased number of free neutrons (protons). The fractionation induced by this effect can be appreciated from Fig. 4, which shows as a function of the fragment size its average isospin content for the four different asymmetries considered above.

The first feature arising from Fig. 4 is that fragments are usually more proton-rich than the corresponding source. The only exception corresponds to the symmetric source and fragments whose charge is close to half the source charge, where mass and charge conservation induces for the Z/A ratios values slightly lower than 0.5. Thus, the approximation frequently invoked in multifragmentation studies—that primary fragments have the same N/Z of their emitting source [22,25,46,47]—does not seem to be correct if primary partitions correspond to statistical equilibrium.

Even more importantly, the degree of fractionation is seen to monotonically increase with the asymmetry of the source, independent of the location of the multifragmentation event in the phase diagram. Indeed, the occurrence of fractionation directly follows from the isospin content of the free particles because of mass and charge conservation; thus, it cannot be taken as a signature of coexistence in finite systems. On the other hand, the behavior of fractionation with fragment size is very different depending on the thermodynamic characterization of the system. Inside the spinodal region (two upper

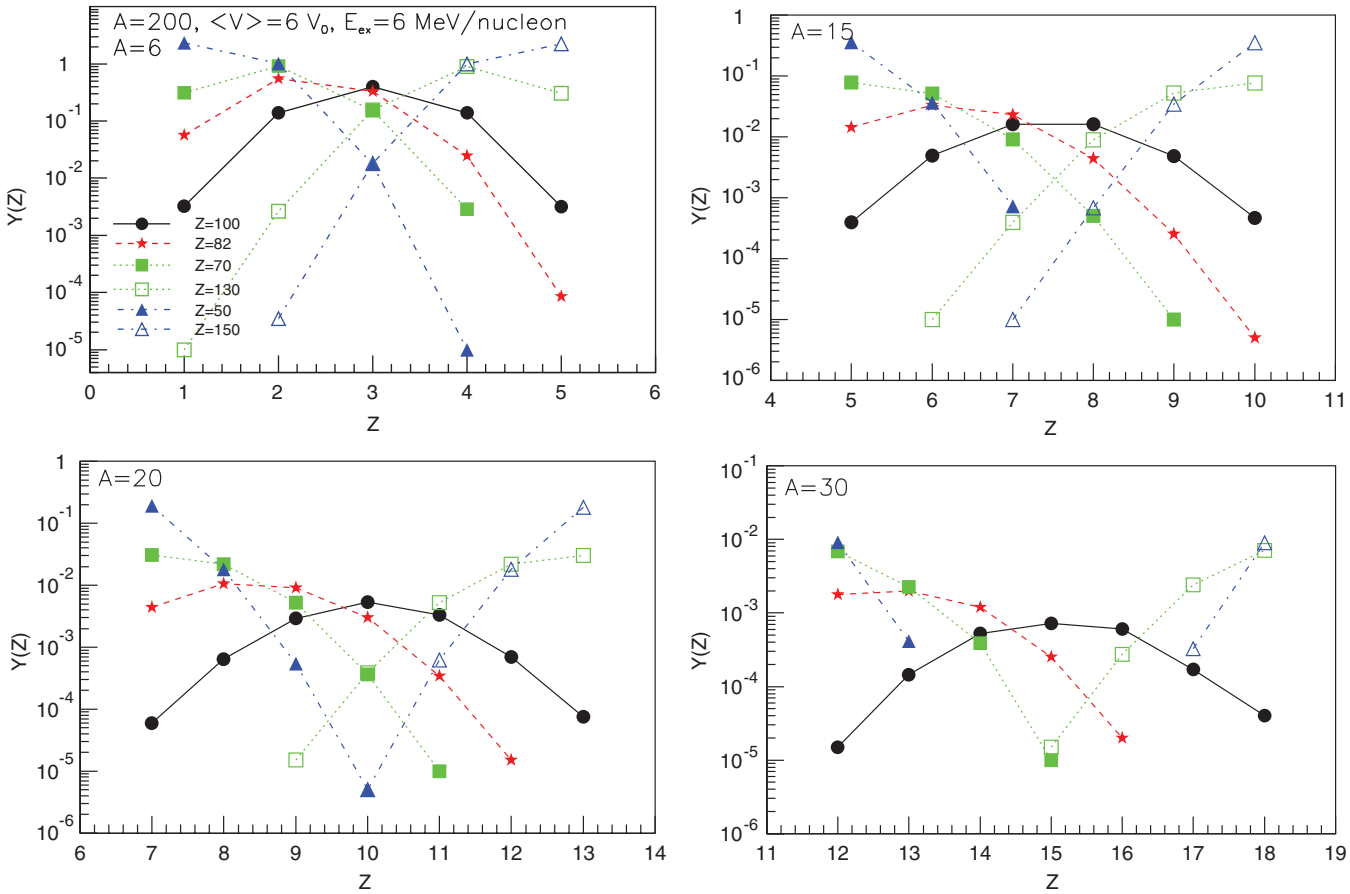

FIG. 3. (Color online) Breakup isotopic yield distributions of isobars with $A = 6$, 15, 20, and 30 originating from the multifragmentation of 200-nucleon sources with different isospin asymmetries at 6 MeV/nucleon excitation energy and an average freeze-out volume $\langle V \rangle = 6V_0$.

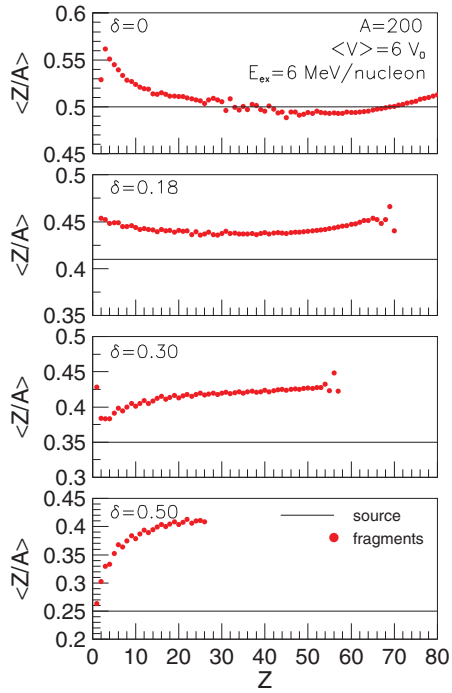

FIG. 4. (Color online) Average isospin content Z/A of the breakup fragments produced in the multifragmentation of different neutron-rich 200-nucleon systems with asymmetries $\delta = 0, 0.18, 0.30, 0.50$ as a function of fragment charge. In all cases, $\langle V \rangle = 6V_0$ and $E_{\rm ex} = 6$ MeV/nucleon. Horizontal solid lines indicate the isospin content of the sources.

panels), the $\langle Z/A \rangle$ vs Z distributions shows a clear U shape, which has already been discussed in Ref. [48]. The two bottom panels, which refer to system in a "pure" phase (liquid or fluid), present similar characteristics which are very different from the behavior discussed above: both show a monotonically increasing $\langle Z/A \rangle$ vs Z distribution, which for $Z_{\rm source}/4$ reaches saturation at about $\langle Z/A \rangle \approx 0.42$.

These observations mean that the fractionation phenomenon naturally appears as soon as the fragmentation process is ruled by thermal laws. It allows one to identify the coexistence region of the first-order phase transition only if an accurate isotopic characterization of all emitted fragments is possible.

The energy and asymmetry dependence of fractionation is further explored in Fig. 5, which gives the evolution with excitation energy of various ratios of light mirror nuclei isotopic yields.

The top panel corresponds to the symmetric source (200,100), and the results indicate that no matter the excitation energy, mirror nuclei are produced with equal probability. The lower panels show that this is not true in asymmetric systems, and the increase in the emission probability for asymmetric light clusters, with respect to combinatorial expectations, increases with the asymmetry of the source. Similar to the results of Fig. 4, these results show that fractionation is mainly dictated by the number of evaporated nucleons in excess, and no special pattern can be distinguished for the events located inside the coexistence region with respect to those

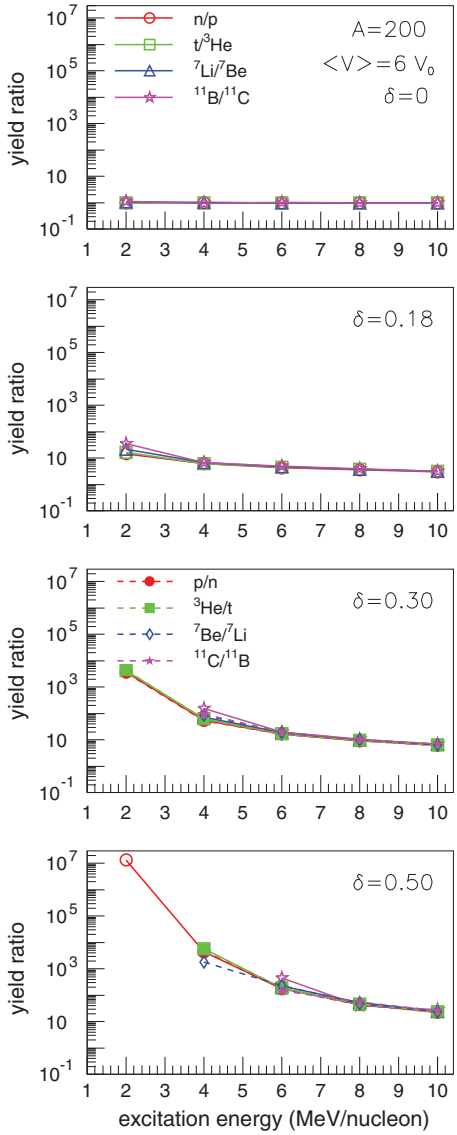

FIG. 5. (Color online) Ratios of isotopic yields of different light mirror nuclei at the breakup stage of 200-nucleon systems with different isospin compositions as a function of excitation energy. In all cases, the average freeze-out volume is $\langle V \rangle = 6V_0$. For the neutron-rich sources, the considered ratios are with the neutron-rich isobars in the numerator; for the neutron-deficient sources, the neutron-rich isobars are in the denominator.

situated in the liquid or supercritical regimes. Indeed, similar values are obtained, for instance, for the $\delta = 0.18$ source with $E_{\rm ex} = 4$ MeV/nucleon (phase coexistence region) and the $\delta = 0.30$ source at $E_{\rm ex} = 8$ MeV/nucleon (supercritical region). Concerning the dependence with excitation energy, we can see that the energy increase partially washes out the trend of the neutron-rich systems to preferentially produce neutron-rich fragments. This is in agreement with statistical microscopic models [49].

Based on the idea of isospin fractionation, it has been proposed that the gas neutron enrichment can be measured from such ratios [19,25]. Indeed, in the grand-canonical approximation, if the charge difference between the two

isobars is $\Delta Z = 1$, the isobaric ratio is given by

$$R = \frac{Y(A, Z_1)}{Y(A, Z_2)} = \exp\left(\frac{\Delta B + \Delta\mu}{T}\right), \quad (2)$$

where $\Delta B = B(A, Z_1) - B(A, Z_2)$, and $\Delta\mu = \mu_n - \mu_p$, if the neutron-rich isobar is in the numerator. Choosing light isobars having close binding energies, this ratio is then a direct measure of the chemical potential difference between neutrons and protons, i.e., of the ratio ρ_n/ρ_p of the free neutron-proton densities.

Figure 5 shows that at least for the considered fragments, this approximation is reasonable enough for all excitation energies and asymmetries, and information on the free neutron vs proton behavior can indeed be inferred from the measurements of isotopically resolved light fragments, assuming that freeze-out yields can be restored from the experimentally detected cold fragments. However, it is important to stress that this free densities ratio cannot unambiguously sign the neutron enrichment of the gas phase, since, as discussed above, the same behavior is observed when no gas phase can be thermodynamically defined.

To conclude, we have pointed out in this section that isospin fractionation cannot be taken as a signature of phase coexistence when dealing with finite systems. In a previous work [24], we already showed that the Coulomb interaction tends to quench the coexistence zone; because of that, the multifragmentation phenomenology can be associated with a supercritical region of the charged-system phase diagram. Here we show that even in the absence of the Coulomb interaction, a generic universal feature of fragmentation, namely, isospin fractionation, can show up above the critical point. If the effect of the Coulomb interaction on the phase diagram strongly depends on the specific model used [24,52], this supercritical fractionation is a generic effect, which we believe should be present in any fragmentation model. Indeed, it is caused by the combined effect of clustering in the supercritical region (which favors the formation of fragments close to stability, i.e., an isospin symmetric fraction of the system condensed at finite baryon density) and particle number conservation (which forces the low-density nonclustered part to have a strong isospin asymmetry). These features are naturally present in any model, microscopic or macroscopic, respecting conservation laws and ruled by the competition between entropy and energy. Such an effect is not accessible in nuclear matter calculations, where the sharing of the system into a dense and a diluted fraction is by construction a sign of phase separation. Classical models [53] have already shown clustering in the supercritical region, but this is to our knowledge the first time that this effect is reported in a realistic nuclear multifragmentation model.

V. ISOTOPIC WIDTHS AND SYMMETRY ENERGY IN FINITE NEUTRAL SYSTEMS

A very powerful motivation in the study of isotopic distributions in fragmentation reactions is given by the well-spread expectation that information coming from the low-density finite-temperature coexistence zone of the phase diagram will be sensitive to the symmetry energy coefficient of the nuclear (free) energy-density functional at finite temperatures and at densities well below saturation [25–29,50]. Such analyses would then be complementary to isospin diffusion and neutron skin measurements [51] and additionally would give unique information on temperature effects on the symmetry energy.

In the MMM model, the binding energy of a cluster of mass A and charge Z is parametrized as

$$\begin{aligned} B_{noC}(A, Z) &= (a_v A - a_s A^{2/3}) - a_i(a_v A - a_s A^{2/3}) \\ &\quad \times \frac{(A-2Z)^2}{A^2} \\ &= (a_v A - a_s A^{2/3}) - C_{\rm sym}(A)\frac{(A-2Z)^2}{A}, \end{aligned} \quad (3)$$

and includes a full mass dependence of the bulk+surface and isospin-dependent contributions. The Coulomb part of the binding energy $(a_c Z^2/A^2 + a_a Z^2/A)$ [54], which is included in the standard version of MMM [23], is switched off for this study, to concentrate on isospin effects.

As we stressed in Sec. II, in the framework of statistical models under the Fisher approximation [35], the low-density correlations are entirely exhausted by clusterization. This means that the symmetry (free) energy entering in the fragment production yields inside coexistence should be the symmetry energy of isolated nuclei at finite temperatures. In particular, the interaction part of this energy [Eq. (3)] should correspond to normal ground-state values, meaning that the liquid-drop parameters a_i, a_v, a_s have standard ground-state values [54]. In our model, isotopic yields are therefore expected to be entirely determined in the whole phase diagram by the symmetry energy coefficients $C_{\rm sym}(A)$.

If this approximation gives a correct description of multifragmentation, this would mean that no relevant information on $C_{\rm sym}(\rho, T)$ can be inferred from fragment observables. If, on the other hand, the energy functional of breakup fragments differs from the ground-state functional [26,27], it would be interesting to trace its behavior, and isotopic distributions could be good candidates. The extent to which this may be true is a difficult theoretical issue, demanding a quantal many-body transport treatment, completely out of the scope of the present study. Whatever the final answer, for the fragment symmetry energy to be accessible from experimental data, it is necessary to prove that in a controlled model where the symmetry energy set in breakup fragments is an input value of the calculation, the proposed observables do indeed recover its value within a good precision.

The information on $C_{\rm sym}$ can be directly inferred from the widths of the isotopic distributions in the grand-canonical approximation. Indeed, a Gaussian approximation on the grand-canonical expression

$$\begin{aligned} Y_{\beta,\mu_n,\mu_p}(N, Z) &= \mathcal{Z}^{-1}_{\beta,\mu_n,\mu_p} \exp\left[-\beta(F_\beta(N, Z) \right. \\ &\quad \left. - \mu_n N - \mu_p Z)\right] \end{aligned} \quad (4)$$

leads to

$$Y_{\beta,\mu_n,\mu_p}(A, N-Z) = K(A)\exp\left[-\frac{(N-Z-I_0)^2}{2\sigma_I^2(A)}\right], \quad (5)$$

where $I_0 = \bar{N} - \bar{Z}$ is the most probable value of $N - Z$ for a given value of the cluster size A, $K(A)$ does not depend on the asymmetry $I = N - Z$, and the isospin variance is related to the symmetry energy coefficient by

$$\sigma_I^2(A) = \frac{AT}{2C_{\rm sym}^{\beta}(A)}. \quad (6)$$

The coefficient $C_{\rm sym}^{\beta}(A)$ appearing in this last expression is a free symmetry energy coefficient given by

$$C_{\rm sym}^{\beta}(A) = \frac{A}{2}\frac{\partial^2 F_\beta(N,Z)}{\partial I^2}|_A, \quad (7)$$

and coincides with $C_{\rm sym}(A)$ defined by Eq. (3) if we neglect the I dependence of the excitation energy and entropy associated with a given mass A. In this case, Eq. (6) reads

$$\sigma_I^2(A) \approx \frac{AT}{2C_{\rm sym}(A)}. \quad (8)$$

The quality of all these approximations can be appreciated from Fig. 6, which displays the width of the asymmetry distribution (open circles) as a function of the fragment mass

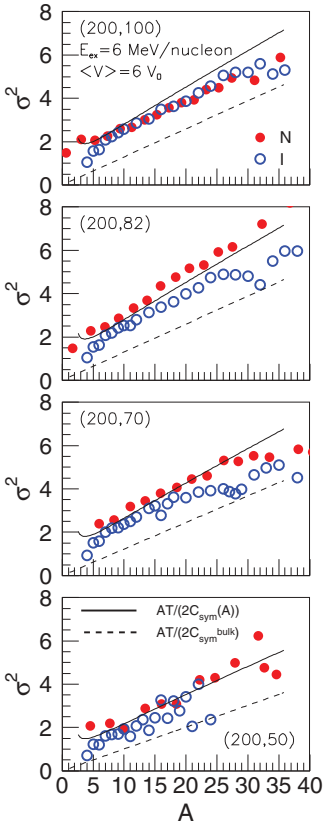

FIG. 6. (Color online) Widths of $Y(I)|_A$ (open symbols) and $Y(N)|_Z$ (solid symbols) distributions corresponding to the breakup stage of 200-nucleon systems with different asymmetries ($\delta = 0$, 0.18, 0.30, 0.50) as a function of fragment mass in comparison with predictions of Eq. (8) calculated for fragment (solid line) and bulk (dashed line) symmetry energies. All systems are characterized by $\langle V \rangle = 6V_0$ and $E_{\rm ex} = 6$ MeV/nucleon, and the Coulomb interaction is switched off.

for the same thermodynamic conditions as Figs. 3–5. For all considered asymmetries, Eq. (8) (solid line) appears well verified for small masses, meaning that this width can indeed be taken as a measure of the underlying symmetry energy. For higher masses and extreme asymmetries, the Gaussian approximation breaks down, as can be observed in Fig. 3, and the link between symmetry energy and fluctuation is lost. The neutron distribution (filled circles) contains approximately the same information brought by the asymmetry distribution. The dashed lines in Fig. 6 give the grand-canonical expectation for the isotopic widths Eq. (8), when only the bulk term ($C_{\rm sym}^{\rm bulk} = a_i a_v$) of the symmetry energy is considered, instead of the complete expression [$C_{\rm sym}(A) = a_i a_v - a_i a_s A^{-1/3}$] used for the solid line. We can see that accounting for surface effects in the fragment energy functional leads to a considerable increase of the isospin widths even for relatively massive fragments. Such fragments ($A \geqslant 30$) are not adapted to the study of the symmetry energy coefficient though, because of the important effect of the mass and charge conservation constraint that causes the widths to deviate from their grand-canonical expectation.

It is very interesting to observe that the solid and dashed lines are almost parallel to each other. This means that the expected functional dependence of the width on the mass number does not change drastically if the symmetry energy has a surface contribution or not. As a consequence, a large width, as expected for light, surface-dominated fragments ($A \leqslant 30$), can be easily misinterpreted as a signature of a reduced bulk symmetry value, as it has been suggested by some recent publications [26,27].

The relation between isotopic widths and symmetry energy has interesting consequences on the isoscaling observable, which has raised great interest in recent literature [16,26,27,50]. As long as the distributions can be approximated by Gaussians, the ratio between the production yield of the same isotope in two different systems (1) and (2) [where we denote by (2) the neutron-rich one] for a given Z can be expressed as a function of neutron number N as

$$\ln\left(\frac{Y_{(2)}(N,Z)}{Y_{(1)}(N,Z)}\right) = -\frac{N^2}{2}\left(\frac{1}{\sigma_{N_{(2)}}^2} - \frac{1}{\sigma_{N_{(1)}}^2}\right) + N\left(\frac{\bar{N}_{(2)}}{\sigma_{N_{(2)}}^2} - \frac{\bar{N}_{(1)}}{\sigma_{N_{(1)}}^2}\right) + K(Z), \quad (9)$$

where $\bar{N}_{(i)}$ is the most probable N value for the element Z in system (i) and $\sigma_{N_{(i)}}^2$ is the variance of the N distribution in the same system. If we choose as systems (1) and (2) two systems of similar masses and temperatures, then $\sigma_{N_{(1)}}^2 \approx \sigma_{N_{(2)}}^2 \approx \sigma_N^2$ and the ratio shows (in log scale) a linear dependence on N (at fixed Z). Similar arguments hold also for fragments with fixed N, meaning that the quantity in the left-hand side of Eq. (9) has also a linear dependence on Z (at fixed N). This result is known in the literature as the isoscaling phenomenon [25]:

$$\ln\left(\frac{Y_{(2)}(N,Z)}{Y_{(1)}(N,Z)}\right) = \alpha(Z)N + K(Z), \quad (10)$$

where

$$\alpha(Z) = \frac{1}{\sigma_N^2}(\bar{N}_{(2)} - \bar{N}_{(1)}), \tag{11}$$

or, for symmetric distributions,

$$\alpha(Z) = \frac{1}{\sigma_N^2}(\langle N\rangle_{(2)} - \langle N\rangle_{(1)}). \tag{12}$$

In the mass region where the Gaussian approximation is well verified and in the absence of Coulomb effects (see Fig. 6),

$$\sigma_N^2(Z) \approx \sigma_I^2(\langle A\rangle(Z)). \tag{13}$$

Then, the isoscaling parameter $\alpha(Z)$ is linked to the fragment symmetry energy by

$$\alpha(Z) \approx \frac{2C_{\rm sym}(\langle A\rangle)}{\langle A\rangle T}(\langle N\rangle_{(2)} - \langle N\rangle_{(1)}), \tag{14}$$

or, equivalently,

$$\alpha(\langle Z(A)\rangle) \approx \frac{2C_{\rm sym}(A)}{AT}(\langle I\rangle_{(2)} - \langle I\rangle_{(1)}). \tag{15}$$

Figure 7 compares the symmetry energy coefficient extracted from Eq. (14) with the input symmetry energy of the model for a representative case. Different average volumes, excitation energies, and asymmetry ratios give similar results. We can see that once again the Gaussian approximation appears well verified for light fragments, and, in that case, isoscaling techniques give a reasonably good measure of the fragment symmetry energy, because this parameter is directly linked to isotopic fluctuations.

A similar expression,

$$\alpha(Z) \approx \frac{4C_{\rm sym}(\langle A\rangle)}{T}\left(\frac{Z^2}{\langle A\rangle_{(1)}^2} - \frac{Z^2}{\langle A\rangle_{(2)}^2}\right), \tag{16}$$

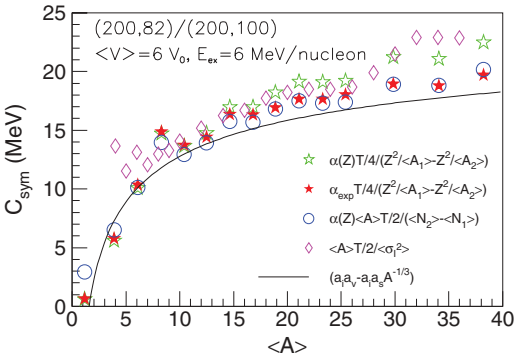

FIG. 7. (Color online) Input symmetry energy coefficient as a function of fragment size (solid line) compared with the estimations from fragment observables, calculated for the breakup stage of (200,82) and (200,100) nuclear systems without Coulomb and with $\langle V\rangle = 6V_0$ and $E_{\rm ex} = 6$ MeV/nucleon. Open diamonds and circles stand for predictions of Eqs. (8) and (14), respectively. Predictions of Eq. (16) are plotted as open or solid stars depending on whether the isoscaling parameter α is calculated according to its definition [Eq. (10)](open stars) or as the average values of fragments with $1 \leqslant Z \leqslant 8$ (solid stars).

was derived in Ref. [16] from Eq. (4) with a similar saddle point approximation as for Eq. (14), considering only the most probable isotopes for each Z. This equation is also plotted in Fig. 7 and gives comparable results to Eq. (14).

In some experimental analyses, the isoscaling parameter $\alpha(Z)$ is not extracted separately for each isotope, as defined in Eq. (10), but as the average value over fragments with $1 \leqslant Z \leqslant 8$. For this last situation, we adopt the notation $\alpha_{\rm exp}$. Figure 7 plots the behavior of Eq. (16) for these different definitions of α. It comes out that the procedure to calculate α using exclusively the light nuclei does not perturb the extracted symmetry energy, but rather minimizes the deformations due to conservation laws, which would prevent a precise extraction of the symmetry energy coefficient for large clusters. Quantitatively speaking, by ignoring the monotonic increase with Z, the use of $\alpha_{\rm exp}$ results in slightly lower values of the symmetry energy with respect to the ones obtained employing $\alpha(Z)$.

It has been recently argued [29,50] that a constant value of the isoscaling parameter α would imply a bulk character for the associated symmetry energy. It is particularly interesting to notice that in our model this is not the case. Indeed, the size dependence of $C_{\rm sym}(\langle A\rangle)/\langle A\rangle$ is compensated by the size dependence of $(\langle N\rangle_{(2)} - \langle N\rangle_{(1)})$ giving a constant α.

VI. ISOTOPIC WIDTHS AND SYMMETRY ENERGY IN REAL NUCLEI

The robustness of these signals to measure the symmetry energy when the Coulomb interaction is included is particularly important, as it gives the extent to which one may extract this basic quantity from multifragmentation data, assuming that one may access the chemical composition of the physically relevant breakup fragments.

In ground-state nuclei, the Coulomb interaction is known to shift the stability peak toward neutron-rich nuclei and to reduce dramatically the binding energy of the proton-rich ones. This last effect is responsible for a strong narrowing of the $B(A, Z)|_A$ and $B(A, Z)|_N$ distributions and becomes more pronounced with the mass increase. Since the logarithm of fragment multiplicity approximately follows the evolution of $B(A, Z)/T$ [Eq. (4)], we can expect to find the same effect of a width reduction on fragment yields.

Figure 8 plots the widths of the $Y(I)|_A$, $Y(N)|_Z$ and, for the sake of completeness, $Y(Z)|_N$ distributions for two nuclei, (210,82) and (190,82), in a thermodynamic state relevant for most multifragmentation reactions, $V = 4V_0$ and $E_{\rm ex} = 6$ MeV/nucleon. The choice of a pair of nuclei with equal charge minimizes the interference between Coulomb and isospin contributions.

We can observe that the expected dispersion between σ_I^2, σ_N^2, and σ_Z^2 increases with the fragment mass and source asymmetry, which obviously restricts the validity of the approximation Eq. (13). The decrease of σ_I^2 and σ_Z^2 can be attributed to the above-mentioned narrowing of $B(A, Z)|_A$ and $B(A, Z)|_N$ distributions under the Coulomb effect. The increase of σ_N^2 then results from particle number conservation. Indeed, under mass and charge conservation, the dispersion of

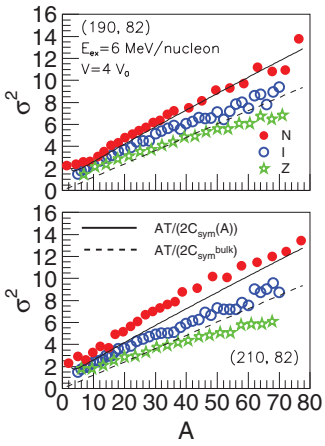

FIG. 8. (Color online) Widths of $Y(I)|_A$ (open circles), $Y(N)|_Z$ (solid circles), and $Y(Z)|_N$ (open stars) distributions corresponding to the breakup stage of two $Z = 82$ nuclei and different asymmetries, $\delta = 0.14$ (upper panel) and 0.22 (lower panel) characterized by $V = 4V_0$ and $E_{ex} = 6$ MeV/nucleon as a function of fragment mass in comparison with predictions of Eq. (8) calculated for fragment (solid line) and bulk (dashed line) symmetry energies.

fragment yields obeys the law:

$$\sigma_I^2 \approx \left(\sigma_N^2 + \sigma_Z^2\right)/2. \tag{17}$$

The consequence of these effects is that the slight deviation of σ_I^2 from Eq. (8), already present for the heavy fragments obtained in the decay of finite neutral systems, becomes more pronounced under the Coulomb effect such that for $A > 50$, σ_I^2 practically falls over the predictions of Eq. (8) with bulk symmetry energy (dashed line) instead of fragment symmetry energy (solid line). However, it is important to observe that for the light fragments which are isotopically resolved in most experimental data sets, σ_I^2 remains an excellent measure of the input symmetry energy irrespective of conservation laws and Coulomb effects.

Finally, Fig. 9 gives the quality of the approximations of the different formulas [Eqs. (8), (14), (15) and (16)] proposed in the previous section to access the symmetry energy. As in

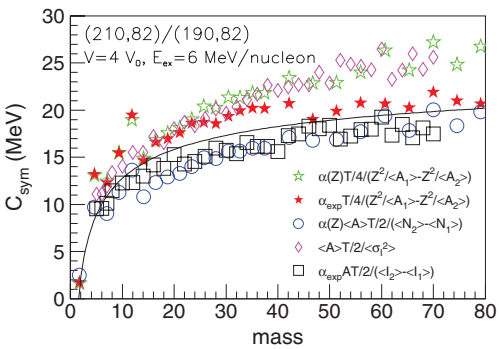

FIG. 9. (Color online) Same as Fig. 7, but for the breakup stage of (210,82) and (190,82) nuclei with $V = 4V_0$ and $E_{ex} = 6$ MeV/nucleon when the Coulomb energy is included. The estimation of Eq. (15) (open squares) is also presented. For this last expression, the abscissa has the meaning of the exact mass.

the previous section, for the so-far widely used Eq. (16) we considered two definitions of α: the slope of the logarithm of isotopic yield ratios for each Z [Eq. (10)] and, in the spirit of most experimental analyses, the average value of $\alpha(Z)$ for fragments with $1 \leqslant Z \leqslant 8$. Not surprisingly, the reconstruction of the input symmetry energy is perturbed by Coulomb effects. As one may notice, for heavy fragments, the violation of the different approximations on which the proposed expressions reckon leads to a relative dispersion which may range from 15% (for $A = 20$) to 25% (for $A = 70$). The best description of the fragment symmetry energy seems to be offered by the simplified version of Eq. (15) where the parameter α is calculated as the average value of Eq. (10) over fragments with $Z = 1-8$ as it underestimates the witness value by less than 1 MeV over the whole considered fragment mass interval ($A = 1 - 70$). As a general statement, considering the light ($A \leqslant 20$) fragments used in most experimental analyses for which the conservation law constraints are the least important, it is encouraging to see that both isoscaling and isotopic widths give a consistent estimation of C_{sym} which deviates from the input value by no more than 20% [55].

VII. CONCLUSIONS

Isospin effects on the thermal and phase properties of finite uncharged excited nuclear systems at subnuclear densities have been studied in the framework of a microcanonical statistical model with cluster degrees of freedom. We find that the isospin asymmetry of the source reduces the width of the coexistence region and the critical temperature and pressure values, in qualitative agreement with well-known results for infinite nuclear matter. The similarity of the phase diagram with the nuclear matter one is an extra confirmation that the multifragment production phenomenon can be associated with the coexistence zone of a first-order phase transition of the liquid-gas type.

To push this connection further, we have explored the relation between fragment chemical composition and the expected isospin fractionation in the coexistence region of a multifluid system. We have shown that a number of excess neutrons are emitted as free particles in neutron-rich sources. This number strongly increases with the asymmetry of the source, independent of the system location in the phase diagram. This implies that free nucleons emitted by a finite isolated system cannot be unambiguously associated with the gas phase of the corresponding phase diagram. Because of the mass and charge conservation law, the isotopic distribution of complex fragments is in turn mainly dictated by the excess free nucleons. Thus the fractionation phenomenon cannot be taken as a measure of phase coexistence. An interesting observable is given by the U shape of the complete Z/A vs Z distribution which appears characteristic of the phase coexistence region, while more simple quantities such as ratios of mirror nuclei give ambiguous results.

Finally, we investigated the relation between fragment symmetry energy and the variance of isotopic distributions. A simple expression relates the symmetry energy with the isospin asymmetry variance, and a new formula is proposed to

calculate the same quantity from isoscaling observables. While they are always accurate enough in the case of finite neutral systems, some of these expressions show sizable deviations in real nuclei under the influence of the Coulomb interaction. The present study, however, suggests that the widths of the isotopic distributions, as well as the isoscaling parameter, can still give a correct estimation of the symmetry energy in physical nuclear multifragmentation data, provided the breakup fragment partitions can be restored from the detected cold fragments.

[1] J. E. Finn *et al*., Phys. Rev. Lett. **49**, 1321 (1982).
[2] G. Bertsch, P. J. Siemens, Phys. Lett. **B126**, 9 (1983).
[3] C. B. Das, S. Das Gupta, W. G. Lynch, A. Z. Mekjian, and M. B. Tsang, Phys. Rep. **406**, 1 (2005).
[4] H. Muller and B. D. Serot, Phys. Rev. C **52**, 2072 (1995).
[5] H. M. Muller, S. E. Koonin, R. Seki, U. van Kolck, Phys. Rev. C **61**, 044320 (2000).
[6] S. J. Lee and A. Z. Mekjian, Phys. Rev. C **63**, 044605 (2001).
[7] T. Sil, S. K. Samaddar, J. N. De, and S. Shlomo, Phys. Rev. C **69**, 014602 (2004).
[8] C. Ducoin, Ph. Chomaz, and F. Gulminelli, Nucl. Phys. **A771**, 68 (2006).
[9] J. M. Lattimer and M. Prakash, Phys. Rep. **333**, 121 (2000).
[10] N. K. Glendenning, Phys. Rep. **342**, 393 (2001).
[11] J. Richert and P. Wagner, Phys. Rep. **350**, 1 (2001).
[12] G. Watanabe and H. Sonoda, in *Soft Condensed Matter: New Research*, edited by F. Columbus (Nova Science, New York, 2005).
[13] D. H. E. Gross, *Microcanonical Thermodynamics: Phase Transitions in Small Systems*, Lecture Notes in Physics, vol. 66 (World Scientific, Singapore, 2001).
[14] Ph. Chomaz and F. Gulminelli, in *Dynamics and Thermodynamics of Systems with Long-Range Interactions*, Lecture Notes in Physics, vol. 602, edited by T. Dauxois *et al*. (Springer, New York, 2002); F. Gulminelli, Ann. Phys. (Paris) **29**, 6 (2004).
[15] Bao-An Li, Phys. Rev. Lett. **85**, 4221 (2000).
[16] A. Ono, P. Danielewicz, W. A. Friedman, W. G. Lynch, and M. B. Tsang, Phys. Rev. C **68**, 051601(R) (2003).
[17] V. Baran, M. Colonna, M. Di Toro, V. Greco, M. Zielinska-Pfabe, and H. H. Wolter, Nucl. Phys. **A703**, 603 (2002).
[18] H. S. Xu *et al*., Phys. Rev. Lett. **85**, 716 (2000).
[19] E. Geraci *et al*., Nucl. Phys. **A732**, 173 (2004).
[20] E. Martin, R. Laforest, E. Ramakrishnan, D. J. Rowland, A. Ruangma, E. M. Winchester, and S. J. Yennello, Phys. Rev. C **62**, 027601 (2000).
[21] D. V. Shetty, S. J. Yennello, E. Martin, A. Keksis, and G. A. Souliotis, Phys. Rev. C **68**, 021602(R) (2003).
[22] A. S. Botvina, O. V. Lozhkin, and W. Trautmann, Phys. Rev. C **65**, 044610 (2002).
[23] Al. H. Raduta and Ad. R. Raduta, Phys. Rev. C **55**, 1344 (1997); **65**, 054610 (2002).
[24] Al. H. Raduta and Ad. R. Raduta, Nucl. Phys. **A703**, 876 (2002); F. Gulminelli, Ph.Chomaz, Al. H. Raduta, Ad. R. Raduta, Phys. Rev. Lett. **91**, 202701 (2003).
[25] M. B. Tsang *et al*., Phys. Rev. C **64**, 054615 (2001).
[26] A. LeFevre *et al*., Phys. Rev. Lett. **94**, 162701 (2005).
[27] D. V. Shetty, S. J. Yennello, A. S. Botvina, G. A. Souliotis, M. Jandel, E. Bell, A. Keksis, S. Soisson, B. Stein, and J. Iglio, Phys. Rev. C **70**, 011601(R) (2004).
[28] M. B. Tsang *et al*., Phys. Rev. C **64**, 054615 (2002).
[29] A. Ono, P. Danielewicz, W. A. Friedman, W. G. Lynch, and M. B. Tsang, Phys. Rev. C **70**, 041604(R) (2004).
[30] T. X. Liu *et al*., Phys. Rev. C **69**, 014603 (2004).
[31] M. Colonna and F. Matera, Phys. Rev. C **71**, 064605 (2005).
[32] W. P. Wen *et al*., Nucl. Phys. **A637**, 15 (1998).
[33] J. Aichelin, Phys. Rep. **202**, 233 (1991).
[34] A. Ono and H. Horiuchi, Prog. Part. Nucl. Phys. **53**, 501 (2004).
[35] M. E. Fisher, Physics **3**, 255 (1967).
[36] A. S. Botvina and I. N. Mishustin, Eur. Phys. J. A **30**, 121 (2006).
[37] D. H. E. Gross, Rep. Prog. Phys. **53**, 605 (1990).
[38] J. P. Bondorf, A. S. Botvina, A. S. Iljinov, I. N. Mishustin, and K. Sneppen, Phys. Rep. **257**, 133 (1995).
[39] S. E. Koonin and J. Randrup, Nucl. Phys. **A474**, 173 (1987).
[40] Ph. Chomaz, F. Gulminelli, and O. Juillet, Ann. Phys. (NY) **320**, 135 (2005).
[41] F. Gulminelli, Ph. Chomaz, and V. Duflot, Europhys. Lett. **50**, 434 (2000).
[42] P. Ring and P. Schuck, *The Nuclear Many Body Problem* (Springer-Verlag, New York, 1980).
[43] D. Vautherin, Adv. Nucl. Phys. **22**, 123 (1996); H. R. Jaqaman, Phys. Rev. C **40**, 1677 (1989).
[44] P. Bonche, S. Levit, and D. Vautherin, Nucl. Phys. **A427**, 278 (1984).
[45] K. A. Bugaev, M. I. Gorenstein, I. N. Mishustin, and W. Greiner, Phys. Rev. C **62**, 044320 (2000).
[46] K. H. Schmidt *et al*., Nucl. Phys. **A710**, 157 (2002).
[47] M. D'Agostino *et al*., Nucl. Phys. **A699**, 795 (2002).
[48] Ad. R. Raduta, Phys. Rev. C **73**, 014606 (2006).
[49] Ph. Chomaz and F. Gulminelli, Phys. Lett. **B447**, 221 (1999).
[50] Bao-An Li and Lie-Wen Chen, Phys. Rev. C **74**, 034610 (2006).
[51] A. W. Steiner and Bao-An Li, Phys. Rev. C **72**, 041601(R) (2005).
[52] M. J. Ison and C. O. Dorso, Phys. Rev. C **69**, 027001 (2004).
[53] X. Campi, H. Krivine, E. Plagnol, and N. Sator, Phys. Rev. C **67**, 044610 (2003).
[54] W. D. Myers and W. J. Swiatecki, Nucl. Phys. **81**, 1 (1966); Ark. Fiz. **36**, 343 (1967).
[55] Ad. R. Raduta and F. Gulminelli, Phys. Rev. C **75**, 024605 (2007).